Torus Breakdown and Chaos in a System of Coupled Oscillators

T. Bakri

12th July 2005

Abstract

In this paper, we consider a simple system of two nonlinearly coupled oscillators using averaging and numerical bifurcation techniques. Assuming the internal resonance 1:2 and the coupling terms having opposite sign we establish the existence of a 2π-periodic solution which undergoes a supercritical Neimark-Sacker bifurcation, yielding a stable fixed symmetric torus. Through one route in the parameter space, we numerically show how the torus gets destroyed by numerically following the changes in the involved manifolds [10]. We detected a cascade of period doubling within the 1:6 resonance tongue yielding a strange attractor. Other periodic regimes present in this system are also studied. It seems these two different regimes interact with each other, yielding yet another type of strange attractor. All this happens quite far from the origin. Most of the results in this region are numerical. Still interesting phenomena were captured by the numerical packages CONTENT[5], AUTO[6] and MATCONT[7] showing the complex character of the dynamics in this simple system of coupled oscillators.

1 Introduction

In this paper we continue the study we initiated in [1]. There we have established with great accuracy, using the method of averaging, that under specific conditions the periodic solution of the system undergoes a Neimark-Sacker bifurcation. The study was focused on how to implement the averaging method to pinpoint efficiently this kind of bifurcations. Also a comparison between the harmonic balance method and averaging was given. The aim of the present article is to study the dynamics after the Neimark-Sacker bifurcation has occurred. We will restrict our study in this paper to the autonomous case i.e. with no parametric excitation. In this case, there is a periodic orbit which undergoes a Neimark-Sacker bifurcation. Unfortunately this bifurcation is not captured by the averaging method as it occurres too far from the origin. Nevertheless a numerical study using the software packages AUTO [6] and CONTENT [5] shows, through one route in the parameter space, how the emerging torus becomes unsmooth before it breaks down. This occurs after the torus becomes resonant and undergoes one period doubling. Due to a cascade of period doublings in the 1:6 resonant tongue, a nontrivial limit set emerges and a strange attractor is born. This is one of the known routes to chaos. Of course there are other scenarios of torus breakdown through other routes in the parameter space which are not covered here. For a detailed analysis of the so far known scenarios of torus breakdown, we refer to Afraimovich and Shilnikov [2] and Shilnikov [3].

After giving a brief description of the equations of motion, we proceed in the next section by studying the flow in the vicinity of the critical points. In section 3, we perform scaling and first order averaging to the equations of motion. We find one periodic orbit of which we analytically determine the stability. Section 4 deals with the numerical study of the original system. We find an attracting torus by a Neimark-Sacker bifurcation. The bifurcation diagram in Figure 5 shows the presence of a 1:6 resonant tongue in the parameter region of our interest. The Poincaré section is examined. It explicitly shows how the torus is destroyed by following the changes in the involved manifolds. Other periodic regimes present in the system are analysed and a bifurcation

diagram is given in section 5. As mentioned above, we explored in our numerical study only one route in the parameter space. In this respect the study is not quite complete, however the results are interesting and somewhat surprising in the way that such a simple system can have such a complex dynamics.
Let's begin by writing down equations of motion:

$$\begin{cases} \ddot{x} + \delta x^2 \dot{x} + x + \gamma x^3 + axy = 0, \\ \ddot{y} + \kappa \dot{y} + 4y + bx^2 = 0. \end{cases} \tag{1}$$

This is a system of two coupled oscillators in 1:2 resonance, nonlinearly coupled. We shall in the numerical study presented here, focus on the case $ab < 0$. In this case one oscillator gets excited by the other through the coupling terms which were chosen as simple as possible.
If $a = 0$, the term $x^2 + \gamma x^3$ represents the restoring force of the x-oscillator. As the bifurcation phenomena, discussed in what follows, take place for small values of γ, we do not expect much different behavior for other restoring forces. For the damping coefficients we have $\delta,\ \kappa \geq 0$, furthermore $\gamma \geq 0$. Adding linear damping to the first oscillator will not affect qualitatively the breakdown scenario described below. We therefore omit it in what follows. Linear damping does however affect the stability of the origin and trigger an extra (unstable) periodic solution. For more details about the origin and the applications of this system, we refer to [1]. For more references on the subject of nonlinearly coupled oscillators see for example [11]. Note that this system possesses a $\mathbb{Z}_2$ symmetry i.e. it is invariant with respect to the transformation:

$$T : \begin{pmatrix} x \\ y \end{pmatrix} \mapsto \begin{pmatrix} -x \\ y \end{pmatrix}.$$

Written as a system of first order ODE's, system(1) becomes:

$$\begin{cases} \dot{x}_1 = x_2, \\ \dot{x}_2 = -x_1 - \delta x_1^2 x_2 - \gamma x_1^3 - a x_1 y_1, \\ \dot{y}_1 = y_2, \\ \dot{y}_2 = -4y_1 - \kappa y_2 - b x_1^2. \end{cases} \tag{2}$$

2 Study of the flow in the vicinity of the equilibria

There are two cases which should be distinguished, namely the case $ab > 0$ and the case $ab < 0$. The case $ab = 0$ is not interesting in our study because then we loose the coupling between the two oscillators. Every motion will end up at the origin because of the damping terms.

2.1 The case $ab > 0$

This case is simple because dynamically speaking no interesting bifurcations occur. Nevertheless we shall give a brief description of the dynamics.
When $ab > 0$ and provided $ab > 4\gamma$, there are three critical points namely:

$$(0,0,0,0), \text{ and } (\pm 2/\sqrt{ab - 4\gamma}, 0, -b/(ab - 4\gamma), 0).$$

The origin has the following eigenvalues:

$$\lambda_{1,2} = \pm\, i,$$
$$\lambda_{3,4} = \frac{-\kappa \pm \sqrt{\kappa^2 - 16}}{2}.$$

So the stability is not conclusive from linear analysis. We shall therefore reduce the flow to the centre manifold and normalise it.

2.2 Centre manifold computation for the origin

For this aim, we consider system (2) in the vicinity of the origin and write it in the following form:

$$\dot{X} = AX + F(X),\ X \in \mathbb{R}^4, \tag{3}$$

where $X = (x_1, x_2, y_1, y_2)^T,\ F(X) = (0, -\gamma x_1^3 - \delta x_1^2 x_2 - a x_1 y_1, 0, -b x_1^2)^T = O(\|x\|^2)$ and

$$A = \begin{pmatrix} 0 & 1 & 0 & 0 \\ -1 & 0 & 0 & 0 \\ 0 & 0 & 0 & 1 \\ 0 & 0 & -4 & -\kappa \end{pmatrix}.$$

In this case A has a simple pair of complex eigenvalues on the imaginary axis: $\lambda_{1,2}$. These are the only eigenvalues of A on the imaginary axis for positive κ as $\lambda_{3,4} = \frac{1}{2}(-\kappa \pm \sqrt{\kappa^2 - 16})$. The usual steps for centre manifold computation are described in [8] chapter 5. We therefore will not go into all the technical details.
In order to reduce the flow to the centre manifold, we use the eigenvectors corresponding to the 'critical' eigenvalues $\lambda_{1,2}$ of the matrix A and its transpose A^T to "project" the system into the 'critical' eigenspace and its complement. Let q be a complex eigenvector corresponding to λ_1. Then we have:

$$Aq = iq,\ A\bar{q} = -i\bar{q}.$$

We introduce the corresponding adjoint eigenvector p such that:

$$A^T p = -ip,\ A^T \bar{p} = i\bar{p}$$

and satisfying the normalisation condition

$$\langle p, q \rangle = 1$$

where $\langle p, q \rangle = \sum_{i=1}^4 \bar{p}_i q_i$ is the standard inner product in $\mathbb{C}^4$. In our case we have

$$q = [-i, 1, 0, 0],\ p = \frac{1}{2}[-i, 1, 0, 0].$$

After some manipulations, and using the polar representation ($z = \rho e^{i\phi}$), the reduced system to the centre manifold is smoothly orbitally equivalent to

$$\begin{cases} \dot{\rho} = & \mathrm{sgn}(l_1(0))\rho^3 + O(\rho^4), \\ \dot{\phi} = & 1 \end{cases} \tag{4}$$

where $l_1(0)$ denotes the first Lyapunov coefficient and is given below

$$l_1(0) = \frac{1}{2}\mathrm{Re}\left[\langle p, C(q, q, \bar{q})\rangle - 2\langle p, B(q, A^{-1}B(q, \bar{q}))\rangle + \langle p, B(\bar{q}, (2iE - A)^{-1}B(q, q))\rangle\right],$$

with

$$B_i(x, y) = \sum_{j,k=1}^{4} \left.\frac{\partial^2 F_i(\xi)}{\partial \xi_j \partial \xi_k}\right|_{\xi=0} x_j y_k,$$

$$C_i(x, y, z) = \sum_{j,k,l=1}^{4} \left.\frac{\partial^3 F_i(\xi)}{\partial \xi_j \partial \xi_k \partial \xi_l}\right|_{\xi=0} x_j y_k z_l,$$

where $i = 1 \cdots 4.$ and E the identity matrix in $\mathbb{R}^4$.

In our case, this reduces to

$$l_1(0) = -\frac{ab}{4\kappa}. \tag{5}$$

Clearly we have $l_1(0) < 0$ in the case $ab > 0$, The origin is hereby nonlinearly locally stable.

The two symmetrical fixed points are of saddle type, the expressions for the eigenvalues are too long to write down explicitly. The phase portrait is roughly sketched in Figure 1 below. When $ab < 4\gamma$ the two symmetrical critical points disappear by going to infinity.

Proposition 1 *When $0 < ab < 4\gamma$ the origin is a global attractor.*

Proof To see this, we introduce the following Lyapunov function

$$V(x_1, x_2, y_1, y_2) = 2x_1^2 + 2x_2^2 + \frac{4a}{b}y_1^2 + \frac{a}{b}y_2^2 + 2ax_1^2y_1 + \gamma x_1^4. \tag{6}$$

Computing the derivative of this Lyapunov function with respect to the time t yields:

$$\frac{dV}{dt} = -4\delta x_1^2 x_2^2 - \frac{2\kappa a}{b}y_2^2$$

Clearly the orbit derivative is negative when $x_1,\ x_2$ and y_2 respectively are not zero. Notice that the Lyapunov function can also be written in the following way

$$V(x_1, x_2, y_1, y_2) = 2x_1^2 + 2x_2^2 + \frac{a}{b}y_2^2 + \left(\frac{\sqrt{ab}}{2}x_1^2 + 2\sqrt{\frac{a}{b}}y_1\right)^2 + \left(\gamma - \frac{ab}{4}\right)x_1^4. \tag{7}$$

We easily see that in the case $ab < 4\gamma$ the Lyapunov function is positive definite. To prove global stability, it is sufficient to show that the second derivative of the Lyapunov function along the orbits changes sing on the manifold $x_1 = y_2 = 0$ and the manifold $x_2 = y_2 = 0$. We have the following expression for the second derivative:

$$\frac{d^2V}{dt^2} = -8\delta x_1 x_2^3 - 8\delta x_1^2 x_2 \dot{x}_2 - \frac{4\kappa a}{b}y_2\dot{y}_2.$$

We distinguish in what follows between the following cases:

Case A $x_1 = 0,\ y_2 = 0,\ x_2 = 0$
In this case the x-oscillator is at rest i.e. $x_1 = x_2 = 0$ for all t and we get for the second derivative the following expression

$$\frac{d^2V}{dt^2} = -\frac{4\kappa a}{b}y_2\dot{y}_2.$$

Clearly $y_2\dot{y}_2$ changes sign along the orbits as it is the derivative of $y_2^2(t)$ and this has a local minimum at 0 because $y_1 \neq 0$ which implies that $y_2(t)$ is not a constant function of the time t.

Case B $x_1 = 0,\ y_2 = 0,\ x_2 \neq 0$
In this case the second derivative along the orbits of the Lyapunov function has the following dominating terms:

$$\frac{d^2V}{dt^2} = -8\delta x_1 x_2^3 - \frac{4\kappa a}{b}y_2\dot{y}_2 = -8\delta x_1 \dot{x}_1^3 - \frac{4\kappa a}{b}y_2\dot{y}_2.$$

Following a reasoning similar to that above, we see that it is impossible in the case $0 < ab < 4\gamma$ to have both x_1 and y_2 to be independent of the time t. we conclude that in this case as well the second derivative of the Lyapunov function changes sign along the orbits tangent to this manifold.

Case C $x_2 = 0,\ y_2 = 0,\ x_1 \neq 0$
In this case the dominating terms of the second derivative are as follows:

$$\frac{d^2V}{dt^2} = -8\delta x_1^2 x_2 \dot{x}_2 - \frac{4\kappa a}{b} y_2 \dot{y}_2.$$

Suppose we hit the manifold at $t = 0$. then we cannot have the following situation: $\dot{x}_2(0) = \dot{y}_2(0) = 0$. To show this we solve the first equation $\dot{x}_2(0) = 0$. This yields

$$y_1(0) = -\frac{1}{a} - \frac{\gamma}{a} x_1(0)^2.$$

The second equation yields:

$$y_1(0) = -\frac{b}{4} x_1(0)^2.$$

Because of the condition $0 < ab < 4\gamma$, we see that it is impossible to have $\dot{x}_2(0) = \dot{y}_2(0) = 0$. From this we conclude that the second derivative of the Lyapunov function changes sign along the orbits crossing this manifold in this case as well. This concludes the proof that the origin is a global attractor. □
These are all the scenarios that can occur in the case $ab > 0$.

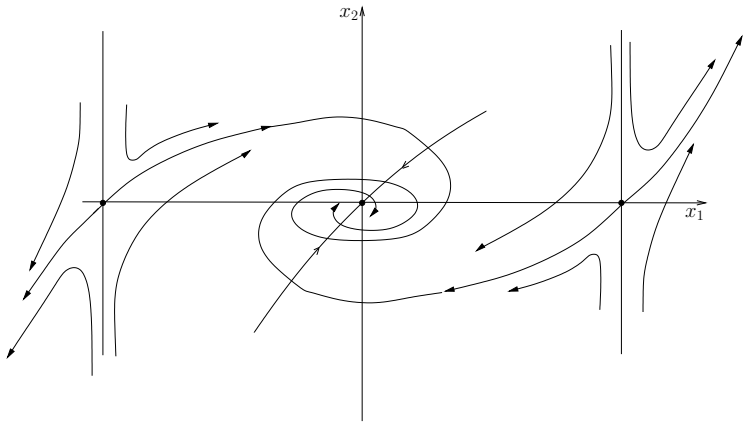

Figure 1: Phase portrait in the case $ab > 4\gamma$

2.3 The case $ab < 0$

When $ab < 0$ the two saddles disappear and the dynamics becomes much richer as we shall see. The origin is in this case nonlinearly unstable as the first Lyapunov coefficient $l_1(0)$ is positive. See equation (5). System (2) is dissipative and because the origin is unstable, one might expect the presence of invariant manifolds. We therefore look first for periodic solutions in the neighborhood of the origin. For this purpose we shall use the method of averaging which enables us to locate periodic solutions and for which precise error estimates are known. To make this more explicit, we introduce the following scaling.

3 Scaling and first order averaging

We consider system (1) in the vicinity of the origin and introduce the following scaling. For more details about this specific scaling see [1].

$$x = \sqrt{\varepsilon}\bar{x},\ y = \sqrt{\varepsilon}\bar{y},\ a = \sqrt{\varepsilon}\bar{a},\ b = \sqrt{\varepsilon}\bar{b},\ \kappa = \varepsilon\bar{\kappa}.$$

The parameters δ and κ are assumed to be $O(1)$ with respect to ε. Introducing this scaling into system (1) and omitting the bars yields:

$$\begin{cases} \ddot{x} + x + \varepsilon a x y + \varepsilon(\delta x^2 \dot{x} + \gamma x^3) = 0, \\ \ddot{y} + 4y + \varepsilon\kappa\dot{y} + \varepsilon b x^2 = 0. \end{cases} \tag{8}$$

The next steps are the usual ones in averaging approximations; see for instance [4], chapter 11. We introduce the following transformation:

$$\begin{cases} x(t) = R_1(t)\cos(t + \phi(t)) & \dot{x}(t) = -R_1(t)\sin(t + \phi(t)) \\ y(t) = R_2(t)\cos(2t + \psi(t)) & \dot{y}(t) = -2R_2(t)\sin(2t + \psi(t)) \end{cases}$$

Averaging the resulting system yields:

$$\begin{cases} \dot{R}_1 &= \varepsilon R_1\{\frac{a}{4}R_2\sin(2\phi - \psi) - \frac{\delta}{8}R_1^2\} \\ \dot{\phi} &= \varepsilon\{\frac{a}{4}R_2\cos(2\phi - \psi) + \frac{3}{8}\gamma R_1^2\} \\ \dot{R}_2 &= \frac{\varepsilon}{2}R_2\{-bR_1^2/(4R_2)\sin(2\phi - \psi) - \kappa\} \\ \dot{\psi} &= \frac{\varepsilon}{2}\{bR_1^2/(4R_2)\cos(2\phi - \psi)\} \end{cases} \tag{9}$$

The dimension of this system can be reduced by introducing the phase variable $\theta = 2\phi - \psi$. The system becomes

$$\begin{cases} \dot{R}_1 &= \varepsilon R_1\{\frac{a}{4}R_2\sin\theta - \frac{\delta}{8}R_1^2\} \\ \dot{R}_2 &= \frac{\varepsilon}{2}R_2\{-bR_1^2/(4R_2)\sin\theta - \kappa\} \\ \dot{\theta} &= \varepsilon\{\frac{a}{2}R_2\cos\theta + \frac{3}{4}\gamma R_1^2 - bR_1^2/(8R_2)\cos\theta\} \end{cases} \tag{10}$$

3.1 The periodic solutions

Equating the right-hand side of system (10) to zero yields the nontrivial critical points of these equations which correspond with 2π-periodic solutions of the original system (8). First, we remark that equating the first two equations to zero and looking for nontrivial solutions is equivalent to the following system:

$$A\begin{pmatrix} R_1^2 \\ R_2 \end{pmatrix} = \begin{pmatrix} 0 \\ 0 \end{pmatrix}$$

with the matrix

$$A = \begin{pmatrix} -\delta/8 & a/4\sin\theta \\ -b/4\sin\theta & -\kappa \end{pmatrix}.$$

If the matrix A is invertible then it is clear that the trivial solution is the only solution. We therefore require that $\det(A) = 0$. A necessary condition for the existence of nontrivial solutions to the reduced system (10) reduces then to

$$\sin\theta = \pm\sqrt{\frac{-2\kappa\delta}{ab}}.$$

Remark

System (10) can have nontrivial equilibrium solutions only if $ab < 0$. One also may assume without loss of generality that $\sin\theta \geq 0$ and $b < 0$. We shall adopt this assumption in what follows.

Solving this system of equations yields:

$$\begin{cases} R_2 &= -\dfrac{b}{4\kappa} R_1^2 \sin\theta \\ R_1 &= \sqrt{\dfrac{-8\kappa^2 \cot\theta}{12\kappa\gamma - ab\sin 2\theta}} \end{cases} \tag{11}$$

provided the damping terms κ, $\delta > 0$. If $\kappa = 0,$ and $\delta \neq 0$ then system (10) has a continuous family of nontrivial critical points and therefore we cannot deduce from this the existence of periodic solutions. However one can easily see from the equations of motion (1) that a family of semitrivial solutions exists. The $x-$oscillator is at rest while the $y-$oscillator is a simple harmonic oscillator. On the other hand, if $\delta = 0,$ and $\kappa \neq 0$ then there is a family of semitrivial solutions where the $y-$oscillator is at rest while the $x-$oscillator oscillates. The period is in this case dependent on the initial condition. System (2) becomes Hamiltonian in the case $\kappa = \delta = 0$. Its Hamiltonian takes the standard structure after the following transformation of coordinates

$$(\tilde{x}_1, \tilde{x}_2, \tilde{y}_1, \tilde{y}_2) = (x_1, bx_2, y_1, \frac{ay_2}{2}).$$

In these new coordinates and omitting the tildes, the Hamiltonian has the following form

$$H(x_1, x_2, y_1, y_2) = \frac{b}{2}\left(x_1^2 + \left(\frac{x_2}{b}\right)^2\right) + \frac{a}{4}\left(4y_1^2 + \left(\frac{2y_2}{a}\right)^2\right) + \frac{\gamma b}{4}x_1^4 + \frac{ab}{2}x_1^2 y_1$$

Conclusion

The original system (8) has an isolated $2\pi-$periodic solution provided γ is large enough, κ, $\delta > 0$ and $\theta \in (\pi/2, \pi)$.

3.1.1 Stability of the $2\pi-$periodic solution

Linearising the reduced averaged system (10) around the nontrivial critical point and analysing the corresponding Routh-Hurwitz system of equations yields that the nontrivial equilibrium is asymptotically stable no matter what the parameters are. This is quite surprising. We refer to the appendix for more details about the stability analysis. This implies that the corresponding periodic solution of system (8) is also asymptotically stable provided its amplitude is $O(1)$. However, using γ as a control parameter, one can numerically see that the amplitudes of the periodic solution R_1 and R_2 can become fairly large and consequently grow beyond the domain of validity of the averaging method. In that case the stability of the periodic solution can be lost due to bifurcations which are not detected by the normal form. We shall therefore return in what follows to the original system (2) and study numerically the flow and the bifurcations involved. This study reveals very rich dynamics including torus break-down, and chaotic behavior as we shall see below.

4 Numerical continuation of the fixed (symmetric) periodic solution

4.1 The Neimark-Sacker bifurcation

The following representative parameters, with respect to the original system (2), have been used in our numerical analysis: $a = 0.5,\ b = -0.5,\ \delta = 0.4,\ \kappa = 0.1$. We use the software package

CONTENT [5] to continue the periodic solution with respect to the parameter γ. Numerical experiments show that interesting phenomena occur for small positive values of the parameter γ; we therefore start at $\gamma = 0.2$ and decrease continuously this parameter. A supercritical Neimark-Sacker bifurcation has been detected at the critical value $\gamma_c \simeq 0.096$. Its normal form coefficient, computed by MATCONT [7] via periodic normalization, is small but negative $C_{NS} = -7.22510^{-7}$. See Figure 2 below. Below but near this critical value of γ a stable smooth torus is present . See the numerically computed Poincaré section in Figure 3. At the parameter value $\gamma = 0.0892$ the torus is destroyed and a strange attractor emerges. See Figure 4. To understand how the torus is destroyed, we first analyse the bifurcation diagram in the involved parameter region.

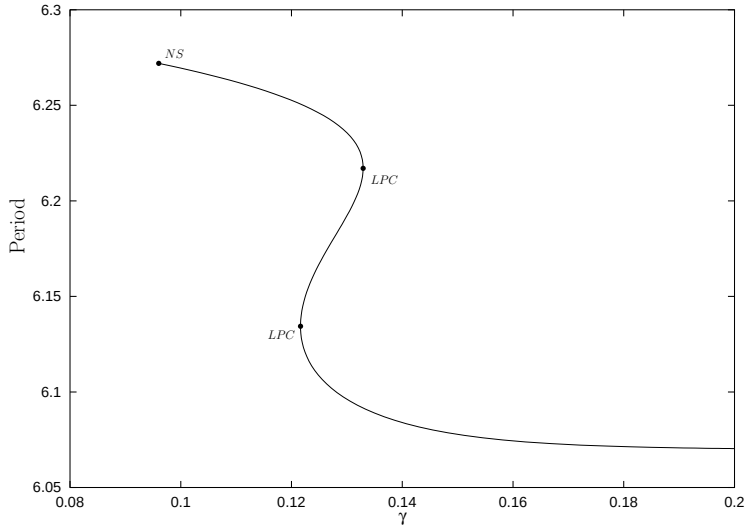

Figure 2: Figure generated by CONTENT. Plot of the period against the parameter γ. The periodic solution is continued with respect to the parameter γ (g on the graphic). LPC stands for Limit Point Cycle (fold) bifurcation and NS stands for Neimark-Sacker bifurcation.

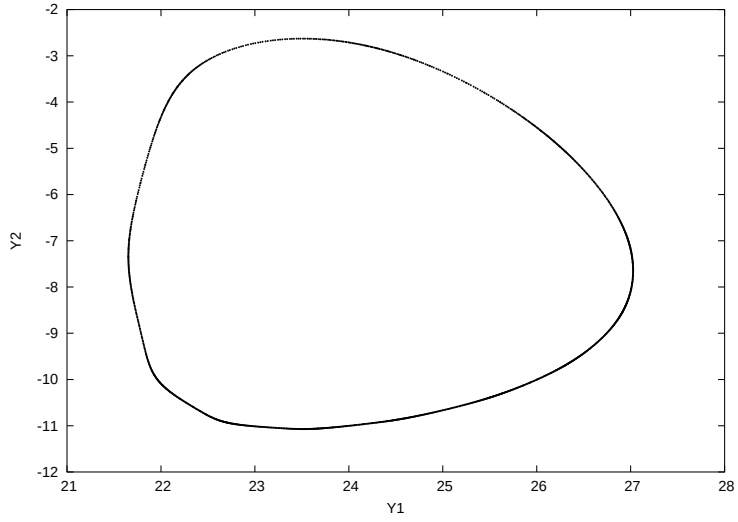

Figure 3: Poincaré section, using $\Sigma = \{(0, x_2, y_1, y_2)^T, x_2, y_1, y_2 \in \mathbb{R}\}$ as cross section, projected onto the $y_1 y_2$ plane with $\gamma = 0.092$. The closed curve corresponds to the stable torus

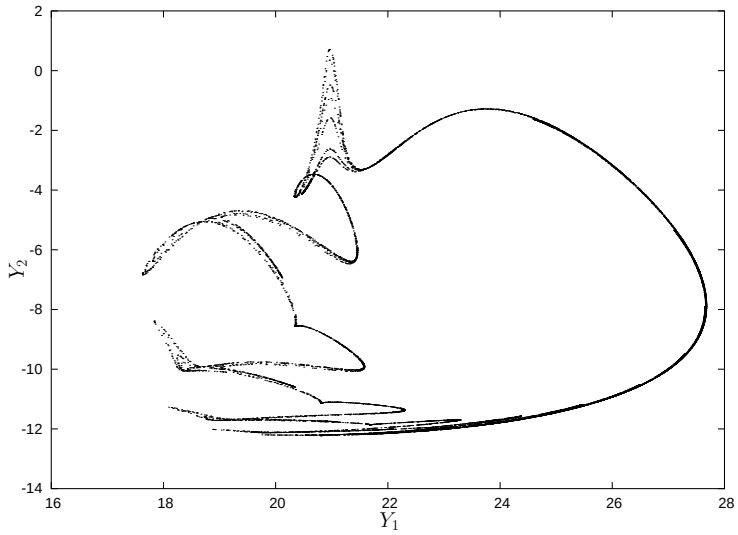

Figure 4: Poincaré section, using $\Sigma = \{(0, x_2, y_1, y_2)^T, x_2, y_1, y_2 \in \mathbb{R}\}$ as cross section, projected onto the y_1y_2 plane with $\gamma = 0.0892$. The closed curve, corresponding with a torus, no longer exists. A strange attractor emerges instead. Kaplan-Yorke dimension $d_{KY} \simeq 2.32$.

4.2 Resonance Tongues and cascade of period doublings

In the parameter region where the smooth torus exists there are regions where phase locking occurs on the torus, the so called Arnold tongues. This happens for example at the parameter value $\gamma = 0.09$ yielding a stable and unstable 1:6 periodic solutions on the surface of the torus. Using the software package AUTO [6] and taking the coupling parameter b as a second control parameter we were able to compute the bifurcation diagram presented below.

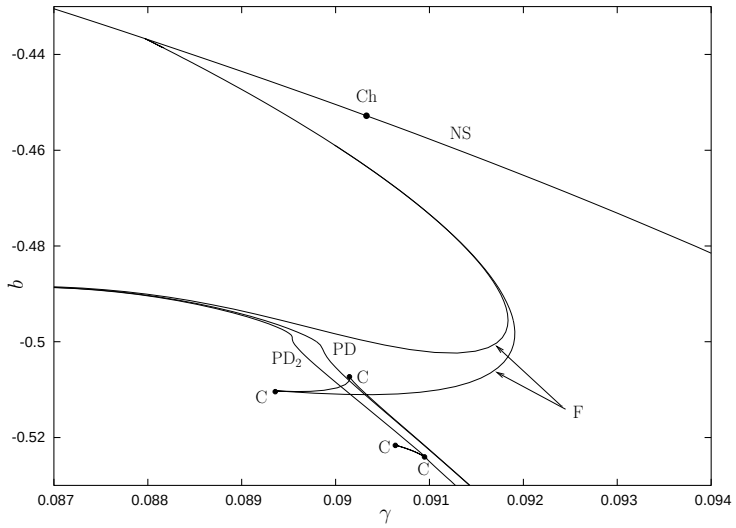

Figure 5: Bifurcation diagram in the case $ab < 0$ in the vicinity of the 1:6 resonance tongue. The tongue is quite narrow and is bounded from below by the period-doubling (PD) curve. The left and right boundaries of the tongue correspond to fold curves (F). Here the period 6 saddle and node solutions collide and disappear. (NS) stands for Neimark-Sacker bifurcation, (Ch) stands for Chenciner bifurcation and (C) corresponds to a cusp bifurcation.

Figure 5 shows part of the bifurcation diagram. The left and right boundaries of the 1:6 resonance tongue correspond to fold curves. There, the saddle and the node collide and disappear. The lower boundary of the tongue corresponds to the first period doubling bifurcation. The stable cycle of period 6 then becomes unstable and a stable period 12 cycle emerges. Because of the symmetry there are two of these cycles. Keeping the parameter $b = -0.5$ constant and letting the parameter γ decrease, we "hit" the 1:6 resonance tongue twice. At the parameter value $\gamma = 0.09184$, further away from the period doubling curve, the Poincaré section shows a smooth closed curve. See Figure 6. As γ decreases, we leave the tongue. The torus is no longer resonant but still smooth. The Poincaré section, in this case, shows a closed curve with no saddles or nodes on it. Entering the tongue for the second time, but now closer to the period doubling curve, at $\gamma = 0.09$ the Poincaré section shows a closed curve which seems to loose its smoothness gradually. See Figure 7. We hit the period doubling curve at exactly the parameter value $\gamma = 0.0897934$. At $\gamma = 0.0897$ i.e. after the first period, the numerically computed Poincaré section shows a closed curve but with complicated geometry. See Figure 8. When γ drops below this critical value, a cascade of period doubling follows respectively at $\gamma = 0.08954709$, $\gamma = 0.08954241$, $\gamma = 0.08954129$ etc. yielding the strange attractor mentioned above. See Figure 4.
One may look at the parameter as a kind of chaos eliminator. Indeed, when the parameter γ equals to zero, the system is either chaotic or its orbits are unbounded. Note that if $a = \gamma = 0$, we have a synchronous oscillator which is a very degenerate case. Introducing the parameter γ and $a > 0$, we couple to an asynchronous oscillator and trigger resonance phenomena which yield the invariant sets we encountered.

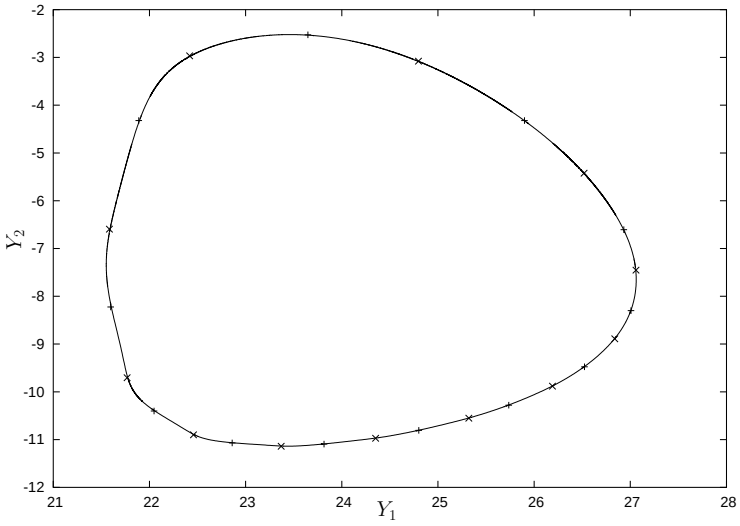

Figure 6: Numerically computed Poincaré section in the 1:6 resonance tongue: $\gamma = 0.09184$. The closed curve is obtained by numerically computing the unstable manifolds of the saddles.

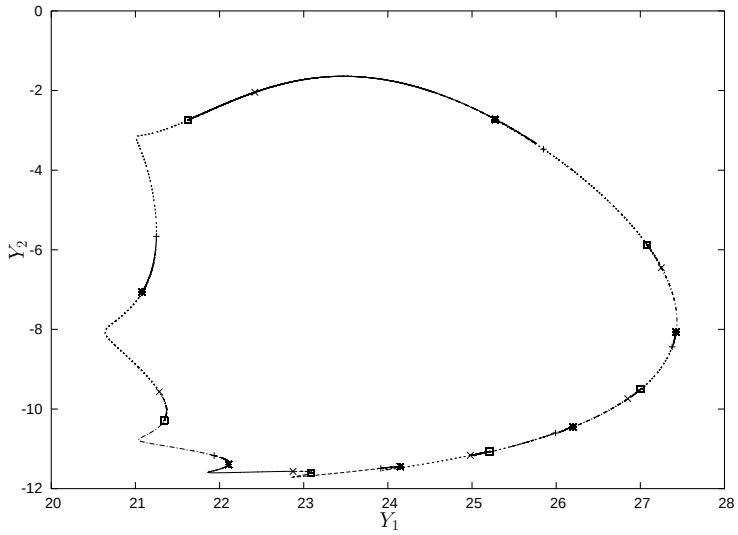

Figure 7: Numerically computed Poincaré section in the 1:6 resonance tongue, closer to the period-doubling curve: $\gamma = 0.09$ showing loss of smoothness.

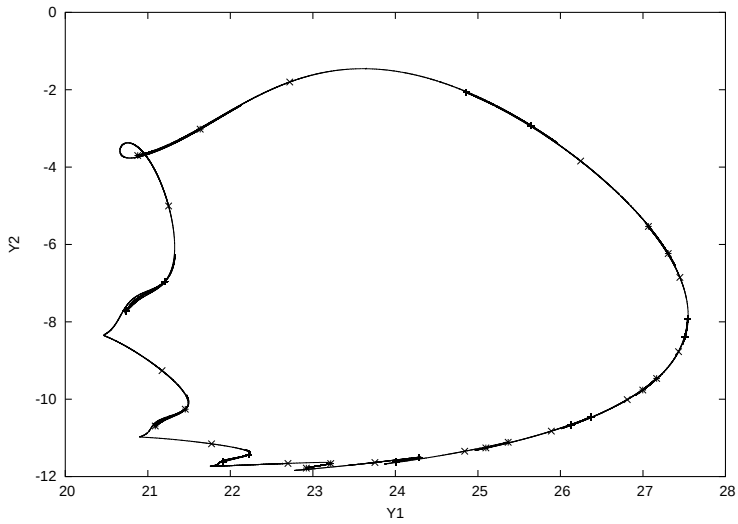

Figure 8: Numerically computed Poincaré section in the 1:6 resonance tongue, after the period-doubling has occurred: $\gamma = 0.0897$.

4.3 Torus destruction

The torus destruction takes place according to one of Afraimovich-Shilnikov scenarios [2]. Let's examine how this happens as a consequence of a period doubling. Before the period doubling takes place, all the four multipliers of the node are positive and are located inside the unit circle. At the period doubling one multiplier becomes equal to -1. Somewhere before this happens the multiplier must become complex. See Figure 7. This means the node becomes a focus. At this stage the closed curve is no longer homeomorphic to the circle. The torus is no longer smooth as the unstable manifold of the saddle winds around the focus infinitely many times. Of course the individual solutions(orbits) remain smooth. After the period doubling has occurred the torus is completely destroyed. See Figure 8 and Figure 9 for a sketch.

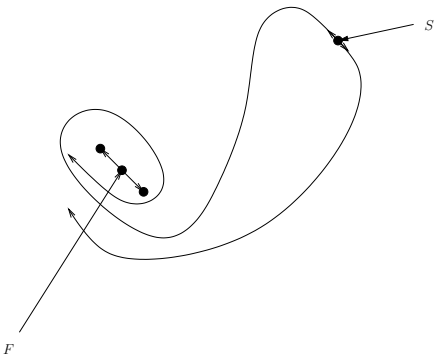

Figure 9: After one period doubling of the fixed point F, the closed curve is no longer homeomorphic to the circle. The torus is completely destroyed.

5 Other regimes

System (1) has other periodic regimes coexisting with the one studied previously. There is a pair of symmetrically coupled $\pi-$periodic solutions. See Figure (10) below.

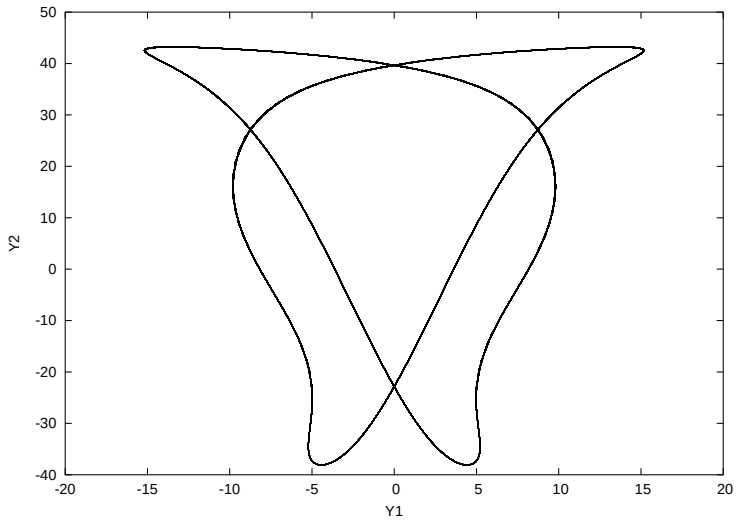

Figure 10: Two symmetrically coupled π-periodic orbits. $\gamma = 0.25$.

A backward continuation of the π-cycle yields a fold bifurcation at $\gamma = 0.23935$ and at $\gamma = 0.25518$, as we hit the left and the right side of the fold curve (**Fold2**) respectively. The stable cycle emerging after the second hit undergoes a Neimark-Sacker bifurcation at $\gamma = 0.23189$ yielding a torus. When we perform a forward continuation of the π-periodic solution with respect to the parameter γ, the cycle undergoes a fold bifurcation at $\gamma = 0.292818$. Here, we hit the curve (**Fold1**). The unstable cycle emerging after this fold bifurcation undergoes a period-doubling bifurcation at $\gamma = 0.119460$. We use, as in section 4.2, the parameter b as a second control parameter to generate the bifurcation diagram. See Figure (11) below.

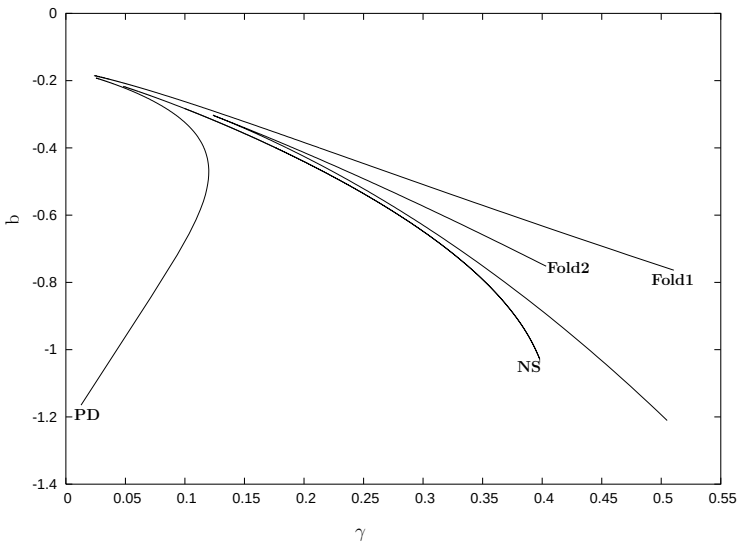

Figure 11: Bifurcation diagram of the π-periodic cycle.

The torus emerging after the Neimark-Sacker bifurcation also becomes resonant and gets destroyed according to a scenario similar to the one described above. Two symmetrically coupled strange attractors are born. If we continue decreasing the parameter γ, the two attractors begin to interact yielding the strange attractor shown in Figure (12) below. One identifies the remains of the two symmetrical tori. The orbits in the strange attractor oscillate randomly between these two objects. This is geometrically reminiscent of the Lorenz attractor.
The 2π unstable cycle emerging from the period doubling bifurcation becomes a neutral saddle at $\gamma = 0.08679$. We suspect this 2π-cycle interacts somehow with the strange attractor in figure 4 yielding also a Lorenz like attractor see figure 13 below. Further study is yet to be done to better understand how the strange attractor evolves and which interactions are involved in this evolution.

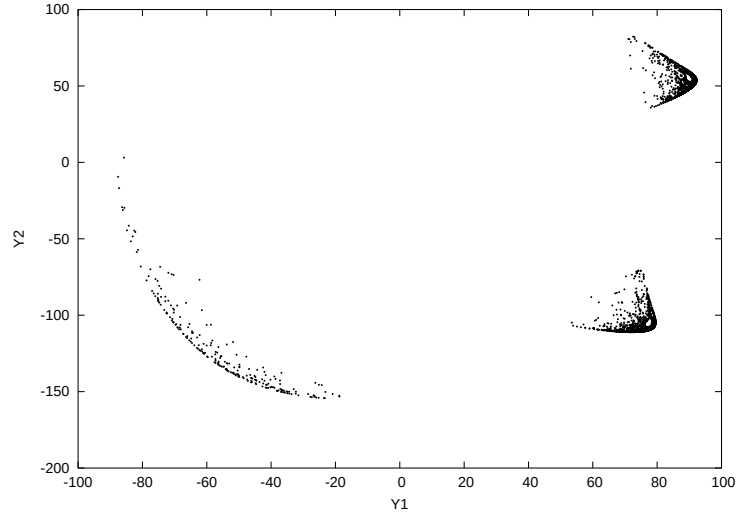

Figure 12: Poincaré section, using $\Sigma = \{(0, x_2, y_1, y_2)^T, x_2, y_1, y_2 \in \mathbb{R}\}$ as cross section, projected onto the $y_1 y_2$ plane with $\gamma = 0.22$. The closed curve no longer exists. A strange attractor emerges instead. Kaplan-Yorke dimension $d_{KY} \simeq 2.90$.

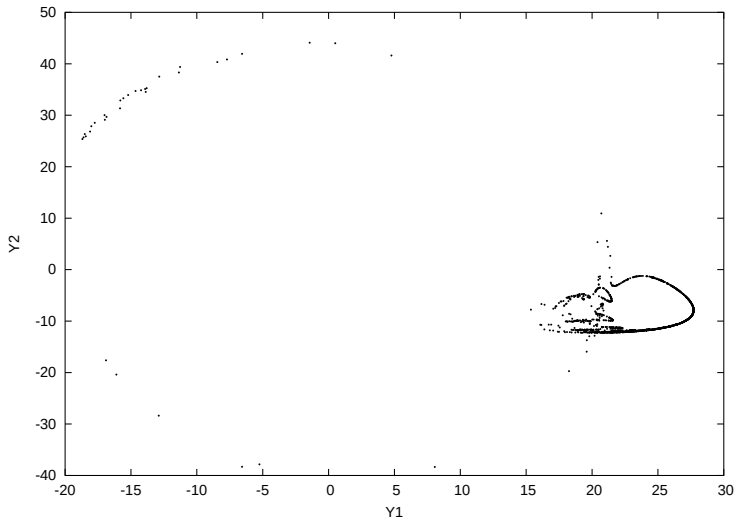

Figure 13: Poincaré section, using $\Sigma = \{(0, x_2, y_1, y_2)^T, x_2, y_1, y_2 \in \mathbb{R}\}$ as cross section, projected onto the y_1y_2 plane with $\gamma = 0.089$. The strange attractor in Figure 4 interacts with other regimes. Kaplan-Yorke dimension $d_{KY} \simeq 2.37$.

6 Acknowledgment

Many thanks to F. Verhulst and Yu.A. Kuznetsov, Mathematics Institute Utrecht University The Netherlands, for their useful remarks.

7 Appendix

7.1 Study of the stability of the periodic solution

Proposition 2 *The nontrivial critical point of system (10) is asymptotically stable everywhere in the parameter space under consideration i.e.* $\kappa,\ \delta,\ a > 0,\ b < 0$.

Proof. We use the Routh-Hurwitz criterion to establish the parameter range within which asymptotic stability holds. A necessary and sufficient condition for asymptotic stability reduces in our case to the following:

$$\begin{cases} \Delta_1 &= \kappa + \dfrac{\delta R_{1a}^2}{2} > 0; \\ \Delta_2 &= -\dfrac{ab}{4\kappa} + \dfrac{\kappa}{16}(ab + 8\delta\kappa)R_{1a}^2 + \dfrac{\delta^2\kappa}{16}R_{1a}^4 - \dfrac{ab\delta^2}{64\kappa}R_{1a}^6 > 0; \\ \Delta_3 &= b_3\Delta_2 > 0. \end{cases} \tag{12}$$

Where,

$$b_3 = \frac{ab\sin 2\theta R_{1a}^4}{256\kappa}(12\kappa\gamma - ab\sin 2\theta).$$

One can easily establish that $b_3 > 0$. This follows from system (11) and the fact that $\theta \in (\pi/2, \pi)$. The first equation is, in our case, automatically satisfied. This way the stability condition reduces to $\Delta_2 > 0$. We will in our proof distinguish between two complementary cases.

The case $ab + 8\delta\kappa \geq 0$

One can easily see from (12) that in this case the second equation is satisfied as all the coefficients of $R_{1a}^{2i},\ i = 0, \cdots, 3$ are positive. This yields asymptotic stability of the nontrivial critical point.

The case $ab + 8\delta\kappa < 0$

We consider here Δ_2 as a function of the parameter γ which is hidden in R_{1a} only and estimate its minimum value with respect to the parameter γ. First We write Δ_2 as follows:

$$\Delta_2 = A - BR_1(\gamma)^2 + CR_1(\gamma)^4 + DR_1(\gamma)^6.$$

Where A, B, C, and $D > 0$ and independent of γ. Taking the derivative with respect to the parameter γ gives:

$$\dot{\Delta}_2 = 2R_1\dot{R}_1(-B + 2CR_1^2 + 3DR_1^4).$$

From equation (11) we see that $\dot{R}_1 < 0$. As $\dot{R}_1 < 0$ and $R_1 > 0$ for all values of γ, we can easily show by analysing the sign of $\dot{\Delta}_2$ that Δ_2, as a function of γ, has one extremum which is a global minimum. We find, after some simplifications, the following expression for the minimum:

$$\Delta_{min} = \frac{-\kappa^2(ab + 2\delta\kappa)}{72a^2b^2\delta}\left(9a^2b^2 + 2ab(Q - 18\delta\kappa) + 12\delta\kappa(Q - 6\delta\kappa)\right),$$

where

$$Q = \sqrt{3(ab + 4\delta\kappa)^2 - 12\delta^2\kappa^2}.$$

Notice that the quantity $-\kappa^2(ab + 2\delta\kappa)/(72a^2b^2\delta)$ is positive in the case $ab + 8\delta\kappa < 0$. It is also easy to show that

$$6\delta\kappa < Q < -\sqrt{3}(ab + 4\delta\kappa)$$

This follows essentially from the fact that $ab + 8\delta\kappa < 0$. With these estimates we can give a lower bound for Δ_{min}. We find

$$\Delta_{min} > \frac{-\kappa^2(ab + 2\delta\kappa)}{72a^2b^2\delta}\left((9 - 2\sqrt{3})a^2b^2 - 2(18 + 4\sqrt{3})\kappa\delta ab\right) > 0$$

This concludes the proof. □

References

[1] T. Bakri, R. Nabergoj, A. Tondl, F. Verhulst, *Parametric Excitation in Non-linear Dynamics*, International Journal of Non-Linear Mechanics 39 (2004) 311–329.

[2] V.S. Afraimovich, L.P. Shil'nikov, *Invariant Two-Dimensional Tori, Their Breakdown and Stochasticity*, Amer. Math. Soc. Trans. (2) Vol. 149, 1991.

[3] A. Shilnikov, L.P. Shilnikov, D. Turaev, *On some mathematical topics in classical synchronisation. A tutorial*, International Journal of Bifurcation and Chaos, Vol. 14,(7) (2004) 2143–2160.

[4] F. Verhulst, *Nonlinear Differential Equations and Dynamical Systems*, Springer, Berlin, Heidelberg, 1996.

[5] Yu.A. Kuznetsov, V.V. Levitin, 1997. CONTENT: A multiplatform environment for analysing dynamical systems. Dynamical Systems Laboratory, Centrum voor Wiskunde en Informatica, Amsterdam, `ftp.cwi.nl/pub/CONTENT`.

[6] E.J. Doedel, R.C. Paffenroth, A.R. Champneys, T.F. Fairgrieve, Y.A. Kuznetsov, B. Sandstede, X. Wang, *Auto 2000: Continuation and Bifurcation Software for Ordinary Differential Equations*. `http://sourceforge.net/projects/auto2000.`

[7] The program MATCONT is freely available for download from:
`http://allserv.rug.ac.be/~ajdhooge`

[8] Yu.A. Kuznetsov, *Elements of Applied Bifurcation Theory*, 2nd Edition, Springer, New York, 1995.

[9] V.I. Arnol'd, *Dynamical Systems V*, Springer, Berlin, 1994.

[10] B. Krauskopf, H. Osinga, *Growing 1D and Quasi-2D Unstabl Manifolds of Maps*, Journal of Computational Physics 146, (1998) 404–419.

[11] R. Lin, C.W.S. To, K.L. Huang, Q.S. Lu *Secondary Bifurcations of Two Non-Linearly Coupled Oscillators*, Journal of Sound and Vibrations (1993) 165(2), 225–250